

Membrane-Spanning Electron Transfer Proteins from Electrogenic Bacteria: Production and Investigation.

Colin W. J. Lockwood, Jessica H. van Wonderen, Marcus J. Edwards, Samuel E. H. Piper, Gaye F. White
Simone Newton-Payne, David J. Richardson, Thomas A. Clarke and Julea N. Butt

Centre for Molecular and Structural Biochemistry, School of Chemistry and School of Biological Sciences, University of East Anglia, Norwich Research Park, Norwich, NR4 7TJ, UK.

Abstract

Certain bacterial species have a natural ability to exchange electrons with extracellular redox partners. This behavior allows coupling of catalytic transformations inside bacteria to complementary redox transformations of catalysts and electrodes outside the cell. Electricity generation can be coupled to waste-water remediation. Industrially relevant oxidation reactions proceed exclusively when electrons are released to anodes. Reduced products such as fuels can be generated when electrons are provided from (photo)cathodes. Rational development of these opportunities and inspiration for novel technologies is underpinned by resolution at the molecular level of pathways supporting electron exchange across bacterial cell envelopes. This chapter describes methods for purification, engineering and *in vitro* characterization of proteins providing the primary route for electron transport across the outer membrane lipid bilayer of *Shewanella oneidensis* MR-1, a well-described electrogenic bacterium and chassis organism for related biotechnologies.

Introduction

Redox enzymes provide attractive renewable electrocatalysts and often deliver performances that match, or exceed, those of their best abiotic counterparts. As a consequence these enzymes provide much inspiration for sustainable energy technologies. Electrocatalysis has been demonstrated for

purified enzymes exchanging electrons with electrodes (Jenner, 2018; Masa & Schuhmann, 2016). Photocatalysis occurs when redox enzymes receive photoenergized electrons (holes) from molecular dyes, (nanostructured) semi-conductors and quantum dots (Bachmeier & Armstrong, 2015; Lee, Choi, Kuk, & Park, 2018). Nevertheless, there are significant bottlenecks to using such approaches for scalable synthesis of high value chemicals, including fuels. Enzyme purification can be costly and time-consuming. Methods to overcome the limited stability of the purified materials may be necessary, for example covalent attachment to solid supports or entrapment in O₂ removing polymers.

The need for protein purification is avoided when using cell-based systems and here the opportunities for electrocatalyst self-repair and regeneration are also attractive (Lapinsonniere, Picot, & Barriere, 2012; Sakimoto, Wong, & Yang, 2016; Saldnoto, Kornienko, & Yang, 2017). Harnessing redox enzyme catalysis in such a context requires a flow of electrons in to, or out from, the cell. For this purpose the outer membrane associated porin:cytochrome complexes and extracellular cytochromes, Fig. 1A, recognized in a growing number of Gram-negative bacteria are highly relevant (Shi et al., 2016; White et al., 2016). These proteins transfer electrons across an otherwise electrically insulating lipid bilayer in natural and engineered bacteria (Schuergers, Werlang, Ajo-Franklin, & Boghossian, 2017) in behavior supporting several energy facing biotechnologies (Bursac, Gralnick, & Gescher, 2017; Fan, Dundas, Graham, Lynd, & Keitz, 2018; Flynn, Ross, Hunt, Bond, & Gralnick, 2010; Logan & Rabaey, 2012; Sasaki et al., 2018; Wang & Ren, 2013). Reductive transformations are driven by electrons entering cells from (photo)cathodes. Oxidized products form exclusively when fermentation delivers excess electrons to (photo)anodes. Furthermore, microbial fuel cells harness electricity produced by bacteria during oxidative waste-water remediation.

[Insert Figure 1 here]

Shewanella oneidensis MR-1 (MR-1) has become a model organism for studying electron transfer across the outer membrane and a chassis for synthetic biology demonstrating proof-of-principle in related biotechnologies due to its genetic tractability, versatile metabolism and phylogenetically

widespread mechanism for electron exchange across the outer membrane (Shi et al., 2016; White et al., 2016). This chapter discusses approaches used by our laboratories to purify, clone, express, engineer and characterize proteins associated with electron exchange across the MR-1 outer membrane.

Purification of the Outer Membrane Spanning MtrCAB Complex from MR-1.

The primary route for electron exchange across the MR-1 outer membrane, Fig. 1A, is provided by the MtrCAB complex (Edwards et al., 2018; Hartshorne et al., 2009). MtrAB spans the lipid bilayer, Fig. 1B left. MtrA contains 10 covalently bound *c*-type hemes and MtrB is predicted to fold as a porin wrapped around MtrA. MtrC contains 10 *c*-type hemes and binds to the extracellular face of the MtrAB porin cytochrome complex, Fig. 1B right. MtrCAB is purified as a stable, tightly-bound heterotrimeric complex from MR-1 grown under (micro-)aerobic conditions in LB supplemented with lactate and Fe(III) citrate as described below. Pure MtrCAB is red in color and displays electronic absorbance typical of the His/His axially ligated, low-spin *c*-type hemes that it contains, Fig. 1C. When resolved by SDS-PAGE using 12 % acrylamide gels and stained with Coomassie dye, Fig. 1D, three clear bands are revealed having apparent masses of approximately ≈ 75 kDa (MtrC), ≈ 65 kDa (MtrB) and ≈ 33 kDa (MtrA).

Triton X-100 is used to solubilize MtrCAB from MR-1 membrane fractions during purification. However, Triton X-100 masks the proteins' absorbance at UV-wavelengths and these detergent micelles usually concentrate alongside MtrCAB producing viscous solutions. As a consequence, pure MtrCAB is exchanged into Fos-Choline-12 for Small Angle Neutron Scattering (SANS) and lauryldimethylamine *N*-oxide (LDAO) for incorporation into liposomes to study electron transfer across a lipid bilayer.

Growth and Harvesting of MR-1: Growth of all liquid cultures is at 30°C with shaking at 200 rpm. A single colony of MR-1 picked from an LB agar plate inoculates 10 mL LB that is cultured overnight. From the resulting culture, 1 mL inoculates 100 mL LB that is cultured overnight. The resulting culture

inoculates 1 L of LB containing 50 mM sodium D, L-lactate and 20 mM Fe(III) citrate having pH = 7.8. Note: the media pH is lowered by the presence of ferric citrate and aliquots of 10 M NaOH must be added to achieve the desired pH. A further overnight culture (\approx 18 hours) is performed during which time iron precipitates can form and these are removed by low-speed centrifugation (500 x *g*, 4°C, 20 min) prior to harvesting the cells by more rapid centrifugation (6,230 x *g*, 4°C, 20 min). The pelleted cells are resuspended and washed in 20 mM HEPES, 50 mM NaCl, pH 7.6 using approximately 15 mL per 1 L of culture. Cells are pelleted by a further round of centrifugation prior to flash-freezing in liquid nitrogen and storage at -20°C.

Membrane Isolation: The cell pellet is thawed during gentle resuspension of cells from 1 L culture in 20 mL of 20 mM HEPES, pH 7.8 containing lysozyme and DNase. When thoroughly resuspended the cells are lysed by two passes through a French press (16,000 psi) then unbroken cells and cell debris are removed by centrifugation (15,000 x *g*, 4°C, 30 min). The membrane fraction (containing inner and outer membranes) is pelleted by ultra-centrifugation (200,000 x *g*, 4°C, 100 min) and resuspended in 20 mM HEPES, 50 mM NaCl, pH 7.8 by gentle stirring overnight (4°C). Addition of 2% (w/v) sodium lauroyl sarcosinate (sarkosyl) over 45 min with gentle stirring (4°C) preferentially solubilizes the inner membrane. Ultra-centrifugation (200,000 x *g*, 4°C, 100 min) produces a red-brown pellet containing predominantly outer membrane and its protein components including MtrCAB. That pellet is solubilized in 30 mL Triton X-100 5% (v/v unless stated otherwise), 20 mM HEPES, pH 7.8 by gentle stirring overnight (4°C). A final round of ultra-centrifugation pellets insoluble material and the red-brown supernatant containing MtrCAB is resolved by chromatography as described below.

Chromatography: The Triton X-100 solubilized MtrCAB containing solution is loaded on to a Q Sepharose column (60 mL) pre-equilibrated with 2% Triton X-100, 20 mM HEPES, 50 mM NaCl pH 7.8 (Buffer A) using a flow rate of 2 mL min⁻¹. After washing the column with 2 column volumes of Buffer A, it is developed with a linear gradient 0 – 50 % of Buffer B (Buffer A with 1 M NaCl) over 800 mL. MtrCAB elutes at \approx 0.2 M NaCl and the corresponding fractions are identified by electronic absorbance

and SDS-PAGE (Fig. 1 C & D). MtrCAB containing fractions are pooled, transferred to dialysis tubing (12 kDa MWCO) and dialyzed against 2% Triton X-100, 20 mM TRIS, 50 mM NaCl, pH 8.5 (Buffer C) overnight (2 x 5 L, 4°C). The dialyzed sample is loaded on to a DEAE Column (130 mL) pre-equilibrated with Buffer C (2 mL min⁻¹). MtrCAB binds to the column, which is washed with Buffer C (2 column volumes) and eluted with a gradient of 0 - 50 % Buffer D (Buffer C + 1 M NaCl). The red fractions containing MtrCAB are pooled and concentrated to < 5 mL. The latter is achieved using either a centrifugal concentrator, or, by loading onto a HiTrap Q Sepharose column (5 mL) equilibrated with Buffer A and eluted with a single step elution to 50 % Buffer B; the column avoids concentration of Triton X-100 that occurs when using spin concentrators.

In the final stage of MtrCAB purification, the concentrated protein (< 5 mL) is passed through a Superdex 200 26/60 column pre-equilibrated with 2% Triton X-100, 20 mM HEPES, 150 mM NaCl, pH 7.8 at a flow rate of 0.5 mL min⁻¹. MtrCAB forms a red band moving through the column and fractions containing the eluted complex should be pure when assessed by SDS-PAGE with Coomassie-stain to visualize total protein. Purified protein is quantified by the electronic absorbance at 410 nm for the oxidized protein using $\epsilon = 2,200 \text{ mM}^{-1} \text{ cm}^{-1}$ assuming each heme has $\epsilon = 110 \text{ mM}^{-1} \text{ cm}^{-1}$. A typical yield is 1 mg MtrCAB per 1 L of culture and samples containing pure MtrCAB are aliquoted and stored at -80°C after flash-freezing in liquid nitrogen.

Detergent Exchange: MtrCAB as purified in Triton X-100 is diluted three-fold with 20 mM HEPES, 50 mM NaCl, pH 7.8 containing the required detergent i.e. 5 mM LDAO (Buffer E), ensuring the final detergent concentration is above the critical micelle concentration. The sample is loaded onto a HiTrap Q-Sepharose column (5 mL) equilibrated with Buffer E. The column is washed with four column volumes (0.5 mL min⁻¹) of Buffer E and the MtrCAB is eluted in a single step with Buffer F (Buffer E + 500 mM NaCl). The resulting sample can be concentrated with a Microcon-30 kDa centrifugal filter (Millipore) without the detergent (LDAO) concentration changing. LDAO, unlike Triton X-100 does not absorb at 280 nm revealing that MtrCAB has $A_{410\text{nm}}/A_{280\text{nm}} \approx 4.5$

Purification of Recombinant MtrAB and MtrC from MR-1

The pBAD202 plasmid (Invitrogen) provides robust access to recombinant proteins in MR-1 (Shi, Lin, Markillie, Squier, & Hooker, 2005). Conferring resistance to kanamycin this plasmid places the gene of interest under control of an arabinose inducible promoter. Recombinant proteins are produced in MR-1 or a desired strain, for example one deficient in the *mtr* operon encoding for MtrCAB, its paralog MtrFED and the extracellular decaheme cytochrome OmcA homologous to MtrC (MtrF), Fig. 2A. We choose the host strain for ease of purification of the desired protein(s) or to facilitate *in vivo* analysis. Various strategies are reported for MR-1 transformation. In our hands the more efficient method is electroporation using a modification of the method of Myers and Myers (Myers & Myers, 1997).

[Insert Figure 2 here]

Electroporation of MR-1. From a single colony of MR-1 on LB agar, a 100 mL LB culture having $OD_{600nm} = 0.4$ (must be < 0.5) is prepared by the method above. Cells are pelleted by centrifugation ($3,220 \times g$, $4^{\circ}C$, 15 min) and the supernatant removed fully to minimize arching during electroporation. The cells are gently resuspended in 8 mL of an ice-cold, filtered solution of 1 M sorbitol and pelleted by centrifugation ($3,220 \times g$, $4^{\circ}C$, 15 min). After removing the supernatant, the cells are gently resuspended in 2 mL of the ice-cold sorbitol solution. Electroporation is performed within 15 min and for this $390 \mu L$ of the cells are added to an ice-cold microcentrifuge tube (1.5 mL) and mixed gently with 0.1 - 0.5 μg of plasmid DNA added in a volume 1-2 μL ; note the DNA should be prepared in sterile molecular biology grade water because arching can occur with too much salt in the sample. The mixture is transferred to an ice-cold 0.2 cm gap electroporation cuvette and treated with a single 1.10 kV pulse (Micropulser Electroporation Apparatus, BioRad) within 15 minutes of adding the DNA. **Immediately** after, 800 μL pre-warmed ($30^{\circ}C$) S.O.C. medium (Sigma-Aldrich) is added to the cuvette and the contents transferred to a 1.5 mL microcentrifuge tube where the cells are allowed to recover at $30^{\circ}C$ for 1.5 -2 hours while shaking at 200 rpm. The cells are pelleted in a microcentrifuge ($4,000 \times g$, room temperature, 5 min) resuspended in 100 μl fresh S.O.C. medium and plated on LB plates

containing 20 $\mu\text{g mL}^{-1}$ kanamycin. Red colonies characteristic of MR-1 typically become visible over 2 days incubation at 30°C.

Purification of Recombinant MtrAB: Recombinant MtrAB proteins, Fig. 2Bi, are produced from a construct prepared by cloning *mtrA* (1002 bp), *mtrB* (2094 bp) and their intergenic region from the genomic DNA of MR-1, into pBAD202 (Edwards et al., 2018). The resulting plasmid (pCL001) when introduced into an *mtr*- MR-1 strain LS329 produces MR-1 strain *mtr**mtrAB*⁺ which accumulates recombinant MtrAB in the outer membrane (Edwards et al., 2018). Purification of MtrAB is facilitated by the absence of other products from the *mtr* operon. SDS-PAGE of pure MtrAB stained by Coomassie dye reveals two bands, Fig. 1E, a tight band at ≈ 75 kDa and a diffuse band at ≈ 33 kDa corresponding to MtrB and MtrA, respectively.

MR-1 strain *mtr**mtrAB*⁺ is grown in M72 media (Casein digest peptone 15 g L⁻¹, papaic digest of soybean meal 5 g L⁻¹, NaCl 5 g L⁻¹) supplemented with 20 mM sodium DL-lactate, 20 mM fumarate, 20 mM HEPES, pH 7.8 and 30 $\mu\text{g mL}^{-1}$ kanamycin. Cultures (1.5 L) are grown at 30°C in 2 L baffled flasks shaken at 200 rpm after inoculation (2 %) with overnight cultures grown aerobically in LB containing 30 $\mu\text{g mL}^{-1}$ kanamycin. In mid-exponential growth ($\text{OD}_{590\text{nm}} \approx 0.6$) induction is by addition of 5 mM L-arabinose at which time shaking is stopped and the cultures left to grow micro-aerobically for a further 18 hr. Cells are harvested by centrifugation (6,230 x g, 4°C, 20 min) washed and resuspended in 20 mM HEPES, 50 mM NaCl, pH 7.8 (Buffer F) using approximately 15 mL per 1 L of culture. Cell pellets are flash-frozen in liquid nitrogen and stored at -20°C until required.

Cell lysis and outer membrane isolation are as described above for purification of MtrCAB aside from preferential solubilization of the inner membrane using 1% (m/v) sarkosyl at 4°C for 45 min. Resolution of proteins in the outer membrane pellet by SDS-PAGE and stained by Coomassie dye shows MtrAB is largely free of contaminating proteins at this stage, Fig. 3A. The outer membrane pellet, Fig. 3B, is solubilized with 20 mL Buffer G (Buffer F + 5% Triton X-100). Resolution of the soluble material by SDS-PAGE and visualization by heme-dependent peroxidase activity reveals that MtrA is the only c-type

cytochrome present in the sample. Further purification of MtrAB follows chromatography as outlined above for purification of MtrCAB. MtrAB elutes from the Q-Sepharose column at ≈ 0.2 M NaCl. The purest MtrAB containing fractions as determined by SDS-PAGE, Fig. 3C, are pooled, dialyzed into Buffer C and loaded on to the DEAE column. MtrAB typically elutes at ≈ 0.16 M NaCl and again the fractions containing pure MtrAB as judged by SDS-PAGE are pooled and concentrated, Fig 3D. At this stage detergent exchange as described above can be carried out if required. This protocol typically yields 0.8 mg MtrAB per 1 L culture, the pure complex (in LDAO) typically has $A_{410\text{nm}}/A_{280\text{nm}} \approx 3.4$ and is quantified using $\epsilon = 1,100 \text{ mM}^{-1} \text{ cm}^{-1}$ at 410 nm for the oxidized protein assuming each heme has $\epsilon = 110 \text{ mM}^{-1} \text{ cm}^{-1}$. Samples containing pure MtrAB are flash-frozen and stored at -80°C .

[Insert Fig 3 Here]

Purification of Recombinant Soluble Forms of MtrC: Genomically encoded MtrC is a lipoprotein transported across the MR-1 outer membrane by the Type II Secretion System (Shi et al., 2008). Replacing the N-terminal acetylation site and native signal sequence of MtrC (MMNAQKSKIALLLAASAVTMALTGC) for the native signal sequence of MtrB allows for secretion of soluble forms of MtrC. These proteins are purified from spent media. Such a construct encoding for C-terminal extension including an enterokinase protease sequence and affinity tags, Fig. 2Bii, typically yields 15 mg MtrC per 1L culture and enabled resolution of this protein's crystal structure by X-ray diffraction (Edwards et al., 2015). LC-MS of recently prepared protein revealed multiple sites of C-terminal cleavage complicating other studies including protein film electrochemistry (Ainsworth et al., 2016; Hwang et al., 2017). We now routinely prepare soluble MtrC^{Strp} from a construct *pJvW001* encoding for a 10 residue C-terminal extension where a two-residue spacer is followed by the Strep II tag Fig. 2Biii. Following purification by affinity chromatography, as described below Fig. 4A, LC-MS of pure MtrC^{Strp} reveals a single mass as anticipated for the Strep II tagged decaheme cytochrome. We note that spent media is loaded directly on to a Strep-tactin XT Superflow column so care must be

taken in the choice of media to minimize the possibility that its components interfere with protein binding.

[Insert Fig 4 Here]

MR-1 containing *pJvW001* is cultured as described above for recombinant MtrAB but with 1 L media in a 2 L baffled flask using 30 mM fumarate. Spent-media containing MtrC^{Strp} is recovered as the supernatant after centrifugation (3,600 x g, 4°C, 20 min). Electronic absorbance of the spent-media supernatant reveals a small peak at 410 nm indicative of the cytochrome superimposed on the absorbance/scatter of media components and lysed cells Fig 4B (grey line and triangles). To each Litre of supernatant, 100 mL of 500 mM NaH₂PO₄, 3 M NaCl, pH 8.0 containing 200 µL biotin blocking solution is added and the pH adjusted to 8. The resulting solution is applied to a Strep-tactin XT Superflow column (5 mL, IBA Solutions for Life Sciences) pre-equilibrated with 50 mM NaH₂PO₄, 300 mM NaCl, pH 8.0 (Buffer H, 1-2 mL min⁻¹). The column turns from white to deep red as MtrC^{Strp} binds, Fig 4C. The loaded column is washed with 10 column volumes of Buffer H and MtrC^{Strp} eluted with 1-2 column volumes of 20 mM biotin in Buffer H (final pH adjusted to 8.0). Columns can be stacked in series to increase capacity if needed. SDS-PAGE of the eluted material stained with Coomassie dye reveals pure MtrC^{Strp}, Fig. 4A lane 5. The protocol typically yields 5-10 mg MtrC^{Strp} per 1 L culture and the protein is exchanged in to the desired biotin-free buffer-electrolyte solution prior to storage at -80°C as flash-frozen aliquots. Samples of pure MtrC^{Strp} typically have $A_{410\text{nm}}/A_{280\text{nm}} \approx 3.6$, Fig. 4B (black line), and are quantified using $\epsilon = 1,260 \text{ mM}^{-1} \text{ cm}^{-1}$ for oxidized protein at 410 nm (Hartshorne et al., 2007). The MtrC crystal structure shows all ten hemes have His/His ligation and as a consequence the electronic absorbance and electron paramagnetic resonance spectroscopies show evidence for only low-spin (and not high-spin) heme (Hartshorne et al., 2008).

Redox Characterization of MR-1 Outer Membrane Cytochromes.

Characteristic changes in the electronic absorbance spectra of the MR-1 outer membrane cytochromes accompany heme reduction, as illustrated for MtrC^{Strp} in Fig. 5A. The Soret band gains

intensity, shifts to longer wavelength and two sharp features appear in the Q-band with maxima at approximately 520 and 550 nm. These properties allow heme reduction potentials to be defined by potentiometric titration monitored by electronic absorbance at visible wavelengths (Hartshorne et al., 2007; Hartshorne et al., 2009). The potential windows encompassing cytochrome redox activity can also be resolved by cyclic voltammetry, Fig. 5B, after adsorption of the proteins as electroactive (sub-)monolayer films on appropriate electrodes (Hartshorne et al., 2007; Hartshorne et al., 2009; Reuillard et al., 2017). Such protein film electrochemistry provides a ready means to assess redox catalysis by these enzymes for example with iron (III) citrate (Hartshorne et al., 2007) and H₂O₂ (Reuillard et al., 2017) as substrates.

[Insert Fig 5 Here]

For MtrCAB we find that quantifying electron transfer across a lipid bilayer is readily achieved after inserting the complex into pre-formed liposomes (Edwards et al., 2018; Hartshorne et al., 2009; White et al., 2013). Homogeneous insertion occurs placing MtrC on the external face of the liposome, Fig. 5C, allowing electron exchange between redox partners located on opposite sides of the bilayer to be quantified by electronic absorbance spectroscopy.

Protein-Protein Interactions

Analysis of the purified MR-1 outer membrane cytochromes by sedimentation equilibrium (SE) analytical ultracentrifugation is particularly valuable for complementing SDS-PAGE and LC-MS by directly measuring the average weight of protein and protein complexes in solution in solution. Samples (≈100 μL) are equilibrated in an 8 cell Ti50 rotor within a Beckman Optima XL-1 Analytical Ultracentrifuge, data analysis performed with Ultrascan II software. The buffer density and partial specific volume (buoyant mass) were determined using the utility software in Ultrascan II.

Analysis of MtrCAB preparations at a range of concentrations and rotation rates revealed that the complex behaved as a single homogeneous species with an apparent molecular mass of ≈ 210 kDa. This implies a 1:1:1 ratio of MtrC, MtrA and MtrB in a heterotrimeric complex (Hartshorne et al., 2009) and is consistent with the SANS envelope of this complex (Edwards et al., 2018). Comparable studies, Fig. 6A, confirm MtrAB, soluble MtrC and soluble OmcA (prepared as described in Edwards et al., 2014) are single homogeneous species with apparent molecular masses of ≈ 119 , ≈ 77 and ≈ 80 kDa respectively in 0.1% Triton X-100, 50 mM $\text{NaH}_2\text{PO}_4/\text{Na}_2\text{HPO}_4$, 50 mM NaCl, pH 7.5. Triton X-100 micelles have an approximate micellar molecular weight of 80 kDa, however the partial specific volume of Triton X-100 is 0.91 mL g^{-1} , which substantially decreases the micellar contribution to the overall mass of the protein complex.

[Insert Fig 6 Here]

A sample containing MtrAB ($0.5 \mu\text{M}$) and an equal concentration of soluble MtrC behaved as a single homogeneous species with apparent molecular mass of ≈ 208 kDa. This mass is comparable to that of native MtrCAB demonstrating the ability of soluble MtrC to reconstitute with recombinant MtrAB to form a single homogeneous species with a 1:1:1 ratio of MtrC, MtrA and MtrB. In contrast, SE of the mixture of equal concentrations ($0.5 \mu\text{M}$) MtrAB and soluble OmcA failed to provide evidence for their association. Resolving the SE profile with a single-component analysis gave an apparent average molecular mass of ≈ 90 kDa, in between those of MtrAB and OmcA. Fitting the data to two non-interacting components gave apparent molecular masses of ≈ 80 and 119 kDa in good agreement with the values resolved for OmcA and MtrAB individually.

Native PAGE, Fig. 6B, confirms and extends the description of protein:protein interactions resulting from SE. Native PAGE is performed with a stacking layer comprised of acrylamide (4%) in 0.2 % Triton X-100, 370 mM Tris-HCl, pH 8.8 above a resolving layer comprised of acrylamide (5%) in 0.2 % (v/v) Triton X-100, 370 mM Tris-HCl, pH 8.8. Samples were incubated on ice for 30 min prior to loading on the gel in a bromophenol blue containing solution of 35% glycerol, 90 mM Tris-HCl, pH 6.8.

Electrophoresis is performed at constant current (15 mA) with a running buffer of 25 mM Tris-HCl, 192 mM glycine, pH 8.4 and proteins are visualized by Coomassie-stain.

MtrAB, MtrC or the soluble form of OmcA (5 μ M) migrate as a single band with the distance of migration increasing as MtrAB < OmcA < MtrC. Thus, the MtrAB complex is stable under the conditions of electrophoresis and the soluble extracellular cytochromes have different charge/size characteristics consistent with their masses and crystal structures (Edwards et al., 2014; Edwards et al., 2015). Mixtures containing 5 μ M MtrAB and OmcA at 2.5, 5 or 10 μ M give rise to two bands. One band migrates to the same extent as OmcA alone and the other band to the same extent as MtrAB alone. This behavior, together with the relative intensities of the bands for each sample, provides no evidence for interactions between MtrAB and soluble OmcA.

Quite different behavior is seen for samples containing MtrAB and soluble MtrC. By itself, MtrC migrates further than MtrAB. However, only one band is resolved for a 1:1 mixture of 5 μ M MtrAB and MtrC and the migration of this band, being slightly faster than MtrAB alone, is different to those of the starting materials. This new band is attributed to formation of an MtrAB-MtrC complex, an interpretation supported by SE and the behavior of samples containing 5 μ M MtrAB and 2.5 or 10 μ M MtrC. Migration of the sample containing 1MtrAB: 0.5MtrC revealed bands corresponding to MtrAB and the MtrAB-MtrC complex. There was no indication of a band migrating as MtrC. However, for 1MtrAB:2MtrC, bands migrating as MtrC and the MtrAB-MtrC complex are resolved with no indication of MtrAB. Taken together, the data support spontaneous formation of a stable, high-affinity 1:1 complex between MtrAB and MtrC under the experimental conditions. The same pattern of behavior was seen using combinations of MtrAB and MtrC^{Strp}. Thus, formation of a high-affinity 1:1 complex of MtrAB and MtrC/MtrC^{Strp} is independent of the nature of the residues in their C-terminal extensions and dependent on the residues present in the native protein.

Conclusion and Prospects

Methods have been described for purification of native and recombinant proteins associated with the primary route for bidirectional electron exchange across the MR-1 outer membrane. Structural, spectroscopic and biophysical studies of the purified proteins have allowed us to reveal their electron transfer properties and structures, in some cases at the atomic level. The stage is now set for rational engineering of *Shewanella* and heterologous hosts to facilitate electronic coupling of internal biotransformations with external (photo-)electrode materials and/or synthetic catalysts. The opportunities to exploit such biohybrids for sustainable technologies contributing to global demands for chemicals, fuels and electricity are wide-ranging.

Acknowledgements

We are grateful to the many colleagues, students and researchers who have enriched our studies of proteins from *Shewanella oneidensis* and related organisms with special thanks Liang Shi, Jim Fredrickson, John Zachara, Lars Jeuken and Erwin Reisner. Financial support is from the UK Biotechnology and Biological Sciences Research Council (K009885, K009753, K010220, L020130, L022176 and L023733 and Doctoral Training Partnership PhD studentship to SEHP) and a Royal Society Leverhulme Trust Senior Research Fellowship to JNB.

References

- Ainsworth, E. V., Lockwood, C. W. J., White, G. F., Hwang, E. T., Sakai, T., Gross, M. A., . . . Butt, J. N. (2016). Photoreduction of *Shewanella oneidensis* extracellular cytochromes by organic chromophores and dye-sensitized TiO₂. *ChemBioChem*, *17*(24), 2324-2333.
- Bachmeier, A., & Armstrong, F. (2015). Solar-driven proton and carbon dioxide reduction to fuels - lessons from metalloenzymes. *Current Opinion in Chemical Biology*, *25*, 141-151.

- Bursac, T., Gralnick, J. A., & Gescher, J. (2017). Acetoin production via unbalanced fermentation in *Shewanella oneidensis*. *Biotechnology and Bioengineering*, *114*(6), 1283-1289.
- Edwards, M. J., Baiden, N. A., Johs, A., Tomanicek, S. J., Liang, L. Y., Shi, L., . . . Clarke, T. A. (2014). The X-ray crystal structure of *Shewanella oneidensis* OmcA reveals new insight at the microbe-mineral interface. *FEBS Letters*, *588*(10), 1886-1890.
- Edwards, M. J., White, G. F., Lockwood, C. W., Lawes, M. C., Martel, A., Harris, G., . . . Clarke, T. A. (2018). Structural modeling of an outer membrane electron conduit from a metal-reducing bacterium suggests electron transfer via periplasmic redox partners. *Journal of Biological Chemistry*, *293*(21), 8103-8112.
- Edwards, M. J., White, G. F., Norman, M., Tome-Fernandez, A., Ainsworth, E., Shi, L., . . . Clarke, T. A. (2015). Redox linked Flavin sites in extracellular decaheme proteins involved in microbe-mineral electron transfer. *Scientific Reports*, *5*, 11677-
- Fan, G., Dundas, C. M., Graham, A. J., Lynd, N. A., & Keitz, B. K. (2018). *Shewanella oneidensis* as a living electrode for controlled radical polymerization. *Proceedings of the National Academy of Sciences of the United States of America*, *115*(18), 4559-4564.
- Flynn, J. M., Ross, D. E., Hunt, K. A., Bond, D. R., & Gralnick, J. A. (2010). Enabling unbalanced fermentations by using engineered electrode-interfaced bacteria. *MBio*, *1*(5), 00190-10.
- Hartshorne, R. S., Jepson, B. N., Clarke, T. A., Field, S. J., Fredrickson, J., Zachara, J., . . . Richardson, D. J. (2007). Characterization of *Shewanella oneidensis* MtrC: a cell-surface decaheme cytochrome involved in respiratory electron transport to extracellular electron acceptors. *Journal of Biological Inorganic Chemistry*, *12*(7), 1083-1094.
- Hartshorne, R. S., Reardon, C. L., Ross, D., Nuester, J., Clarke, T. A., Gates, A. J., . . . Richardson, D. J. (2009). Characterization of an electron conduit between bacteria and the extracellular environment. *Proceedings of the National Academy of Sciences of the United States of America*, *106*(52), 22169-22174.

- Hwang, E. T., Orchard, K. L., Hojo, D., Beton, J., Lockwood, C. W. J., Adschiri, T., . . . Jeuken, L. J. C. (2017). Exploring step-by-step assembly of nanoparticle: cytochrome biohybrid photoanodes. *ChemElectroChem*, 4(8), 1959-1968.
- Jenner, L. P. & Butt, J. N. (2018). Electrochemistry of surface-confined enzymes: Inspiration, insight and opportunity for sustainable biotechnology. *Current Opinion in Electrochemistry*, 8, 81-88.
- Lapinsonniere, L., Picot, M., & Barriere, F. (2012). Enzymatic versus microbial bio-catalyzed electrodes in bio-electrochemical systems. *ChemSusChem*, 5(6), 995-1005.
- Lee, S. H., Choi, D. S., Kuk, S. K., & Park, C. B. (2018). Photobiocatalysis: activating redox enzymes by direct or indirect transfer of photoinduced electrons. *Angewandte Chemie-International Edition*, 57(27), 7958-7985.
- Logan, B. E., & Rabaey, K. (2012). Conversion of wastes into bioelectricity and chemicals by using microbial electrochemical technologies. *Science*, 337(6095), 686-690.
- Masa, J., & Schuhmann, W. (2016). Electrocatalysis and bioelectrocatalysis - Distinction without a difference. *Nano Energy*, 29, 466-475.
- Myers, C. R., & Myers, J. M. (1997). Replication of plasmids with the p15A origin in *Shewanella putrefaciens* MR-1. *Letters in Applied Microbiology*, 24(3), 221-225.
- Reuillard, B., Ly, K. H., Hildebrandt, P., Jeuken, L. J. C., Butt, J. N., & Reisner, E. (2017). High performance reduction of H₂O₂ with an electron transport decaheme cytochrome on a porous ITO electrode. *Journal of the American Chemical Society*, 139(9), 3324-3327.
- Sakimoto, K. K., Wong, A. B., & Yang, P. D. (2016). Self-photosensitization of nonphotosynthetic bacteria for solar-to-chemical production. *Science*, 351(6268), 74-77.
- Saldrnoto, K. K., Kornienko, N., & Yang, P. D. (2017). Cyborgian material design for solar fuel production: the emerging photosynthetic biohybrid systems. *Accounts of Chemical Research*, 50(3), 476-481.

- Sasaki, K., Sasaki, D., Kamiya, K., Nakanishi, S., Kondo, A., & Kato, S. (2018). Electrochemical biotechnologies minimizing the required electrode assemblies. *Current Opinion in Biotechnology*, *50*, 182-188.
- Schuerger, N., Werlang, C., Ajo-Franklin, C. M., & Boghossian, A. A. (2017). A synthetic biology approach to engineering living photovoltaics. *Energy & Environmental Science*, *10*(5), 1102-1115.
- Shi, L., Deng, S., Marshall, M. J., Wang, Z. M., Kennedy, D. W., Dohnalkova, A. C., . . . Fredrickson, J. K. (2008). Direct involvement of type II secretion system in extracellular translocation of *Shewanella oneidensis* outer membrane cytochromes MtrC and OmcA. *Journal of Bacteriology*, *190*(15), 5512-5516.
- Shi, L., Dong, H. L., Reguera, G., Beyenal, H., Lu, A. H., Liu, J., . . . Fredrickson, J. K. (2016). Extracellular electron transfer mechanisms between microorganisms and minerals. *Nature Reviews Microbiology*, *14*(10), 651-662.
- Shi, L., Lin, J. T., Markillie, L. M., Squier, T. C., & Hooker, B. S. (2005). Overexpression of multi-heme C-type cytochromes. *Biotechniques*, *38*(2), 297-299.
- Wang, H. M., & Ren, Z. Y. J. (2013). A comprehensive review of microbial electrochemical systems as a platform technology. *Biotechnology Advances*, *31*(8), 1796-1807.
- White, G. F., Edwards, M. J., Gomez-Perez, L., Richardson, D. J., Butt, J. N., & Clarke, T. A. (2016). Mechanisms of bacterial extracellular electron exchange. *Advances in Bacterial Electron Transport Systems and Their Regulation*, *68*, 87-138.
- White, G. F., Shi, Z., Shi, L., Wang, Z. M., Dohnalkova, A. C., Marshall, M. J., . . . Clarke, T. A. (2013). Rapid electron exchange between surface-exposed bacterial cytochromes and Fe(III) minerals. *Proceedings of the National Academy of Sciences of the United States of America*, *110*(16), 6346-6351.

Key words: cytochrome, electron transfer, *Shewanella*, Heme, Redox Enzyme, Microbial Fuel Cell, Microbial Electrosynthesis

Figure 1.

Schematic of the MtrCAB complex [A] within the outer membrane (green) of MR-1, with the lipid modification of MtrC implied as a black 'tail'. Arrows represent the bi-directional flow of electrons across the membrane, which has the potential to be exploited for biotechnology (see text). Molecular envelopes [B] of MtrAB and MtrCAB resolved by SANS (Edwards et al., 2018) showing their proposed orientation within the outer-membrane. The crystal structure of MtrC (PDB, 4LM8) positioned within (using SUPCOMB) the MtrCAB envelope, secondary protein structure is shown in red and the 10 c-type hemes in blue/grey spheres. UV-Visible absorption spectra [C] of air-oxidized 5 μ M MtrCAB (black), MtrAB (broken line) and MtrC (grey) in 50 mM HEPES, 50 mM NaCl, 5 mM LDAO, pH 7.8. Coomassie stained SDS-PAGE gels [D] of MtrCAB, MtrAB and MtrC^{strp} as indicated with molecular weight markers on left.

Figure 2.

Organization of MR-1 *mtr* gene locus [A] with genes for extracellular cytochromes (red) and porin:cytochrome components (black) with predicted promoters (bent arrows) and terminators (dotted boxes). Schematic [B] highlighting key features of recombinant r i) MtrAB ii) MtrC, iii) MtrC^{strp}, see text for details.

Figure 3.

SDS-PAGE gels [A] showing the purification of recombinant MtrAB. Proteins visualized by Coomassie stain (left) and heme-dependent peroxidase activity (right). Lanes (1) the soluble protein supernatant

and (2) membrane pellet from first ultra-centrifugation, (3) supernatant containing Sarkosyl solubilized inner membrane and (4) outer membrane pellet containing MtrAB from the second ultracentrifugation. Photograph [B] of the membrane pellets (left) and supernatant (right) for the first (top) and second (bottom) ultracentrifugation steps. Coomassie-stained SDS-PAGE gels resolve chromatographic purification of recombinant MtrAB by Q Sepharose [C] followed by DEAE [D] columns. Lanes show Triton X-100 solubilized outer-membrane pellet (PC) and fractions eluted with increasing NaCl concentration, those fractions carried forward from the Q Sepharose column are highlighted.

Figure 4.

Coomassie stained SDS-PAGE gel (4-20 %) illustrating [A] production of MtrC soluble forms: MtrC^{Strp} and MtrC, see text for details. Lanes 1) cells pre-induction; 2) cells post-induction; spent-media after pelleting cells 3) 2x concentrated and 4) 20x concentrated; 5) Pure MtrC^{Strp} eluted from Strep-tactin XT column. Electronic absorbance spectra [B] of spent media concentrated 2x (grey continuous line, panel A, lane 3) and pure MtrC^{Strp} (black continuous line, panel A, lane 5). The spectrum shown by triangles is that of MtrC^{Strp} in spent media obtained by subtracting the spectrum of fresh media and normalizing to that of the pure protein at 550 nm. Photograph [C] of Strep-tactin XT column saturated with red MtrC^{Strp}.

Figure 5.

Electronic absorbance spectra [A] of oxidized (continuous line) and sodium dithionite reduced (broken line) MtrC^{Strp}. Baseline-subtracted cyclic voltammogram of MtrCAB [B] adsorbed on a basal-plane graphite electrode, recorded at 30 mV s⁻¹, 0°C with 3 krpm electrode rotation. Oxidative and reductive peaks, normalized to their respective peak currents. Cartoon [C] showing liposome with MtrCAB embedded, arrow showing bi-directional electron transfer between exterior to the interior compartment and relevant redox partners.

Figure 6.

Sedimentary equilibrium analysis [A] of MtrAB association with MtrC and OmcA at 8 krpm. Absorbance profiles of 0.5 μ M MtrC (squares), 0.5 μ M MtrAB (circles) measured at 410 nm and 0.5 μ M MtrC + 0.5 μ M MtrAB (triangles) measured at 425 nm, (left) and 0.5 μ M OmcA (squares) 0.5 μ M MtrAB (circles) and 0.5 μ M OmcA + 0.5 μ M MtrAB (triangles) measured at 410 nm. The data is fitted to single species (lines) with residual differences between the experimental data and fitted curves shown above and offset for clarity. Native-PAGE gels [B] resolving samples of MtrAB, OmcA and MtrC (Left) and MtrAB, MtrC and MtrC^{Strp} (right) in isolation and after mixing, as indicated, protein visualized by Coomassie stain. Individual proteins at 5 μ M and mixtures contained 5 μ M MtrAB and either 2.5, 5 or 10 μ M OmcA, MtrC or MtrC^{Strp}, as indicated by the molar ratios, in 20 mM HEPES, 50 mM NaCl, 5 mM LDAO, pH 7.2.

Figure 1

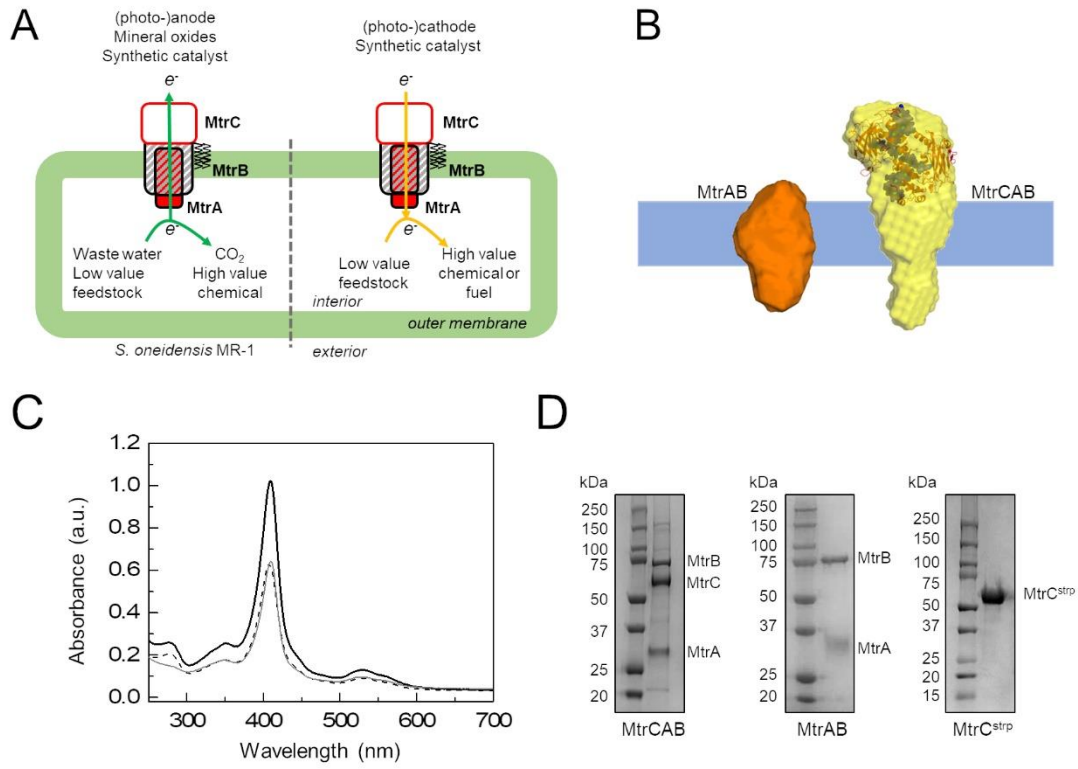


Figure 2

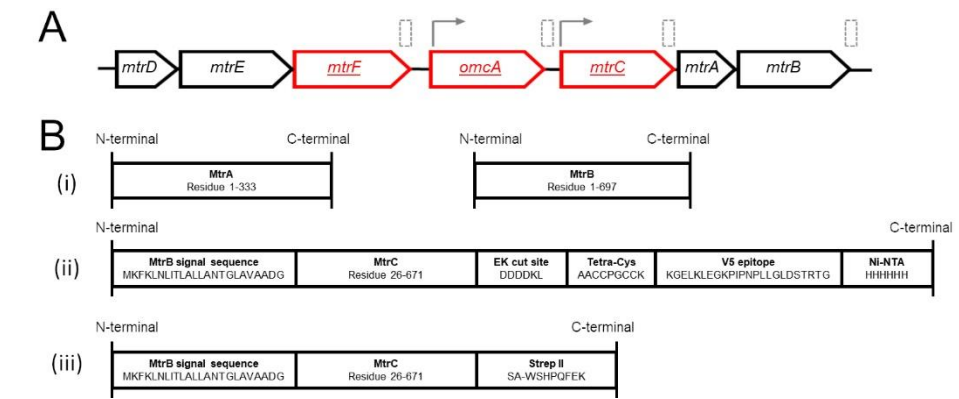


Figure 3

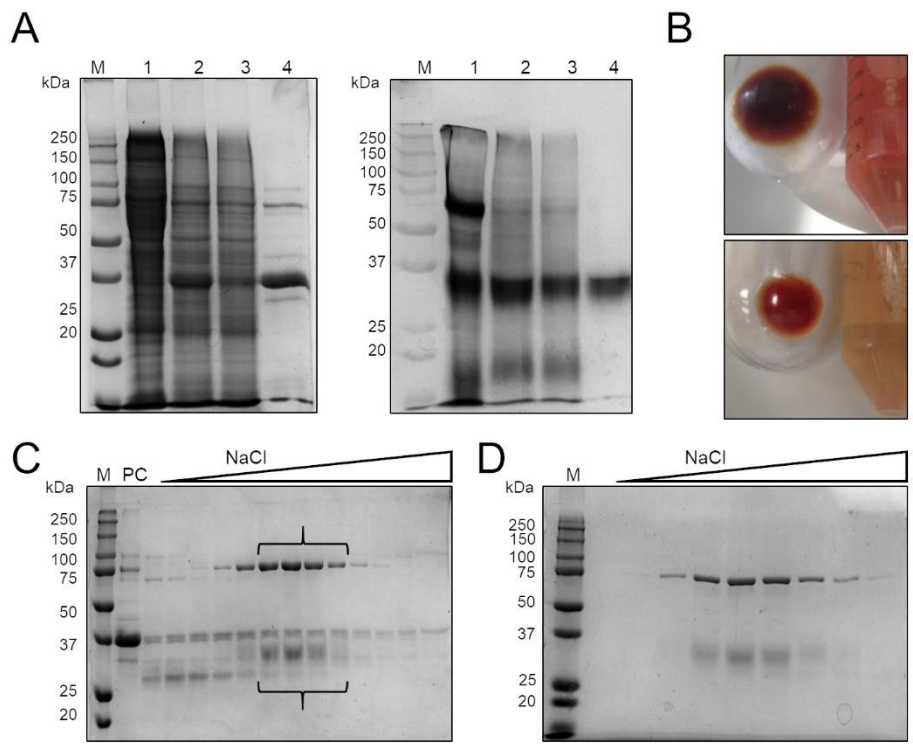


Figure 4

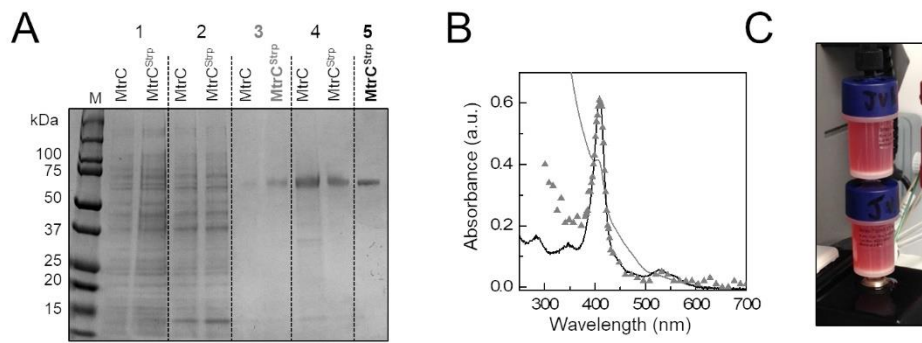


Figure 5

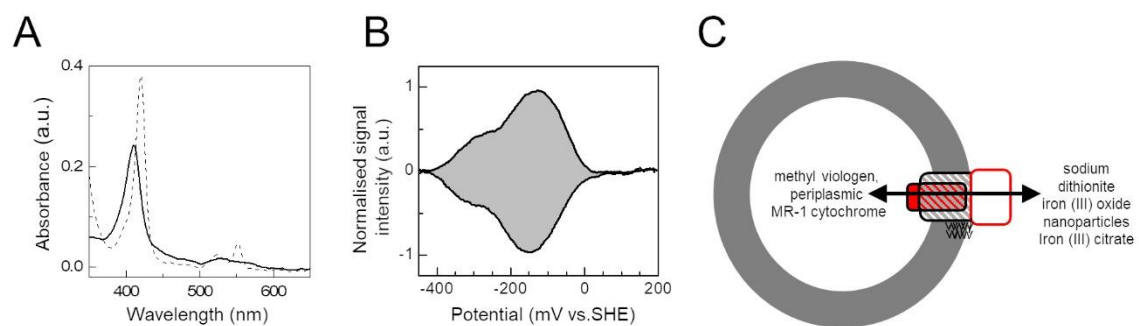


Figure 6

